Article no. 26

THE CIVIL ENGINEERING JOURNAL 3-2020

DYNAMIC CONSTRUCTION CONTROL METHOD FOR A DEEP FOUNDATION PIT WITH SAND-PEBBLE GEOLOGY

Xuansheng Cheng[1], Bingbing Luo[1], Haibo Liu[1], Qingchun Xia[1] and Chaobo Chen[2]

1. *School of Civil Engineering, Lanzhou University of Technology, Lanzhou, No. 287, Langongping Road, 730050, China; chengxslut@sina.com, 2031663951@qq.com, 2459612631@qq.com, 278962530@qq.com*
2. *China Railway 21st Bureau Group Co., LTD., No. 921, Beibinhe West Road, Lanzhou, China; 694874282@qq.com*

ABSTRACT

Taking the water-rich sand and pebble geology deep foundation pit of Jinfu Station of Chengdu Metro Line 6 as the research object, combined with the ladder excavation method of slotting, utilizing finite difference software FLAC 3D as well as on-site monitoring result, the deformation law of the diaphragm wall during the dynamic excavation of the foundation pit is analysed, and the influence of the relative stiffness between the vertical and horizontal walls of the foundation pit on the lateral deformation of the retaining structure is discussed. The results show that while using the ladder excavation method of slotting, the maximum lateral displacement of the underground diaphragm walls decreases gradually with the excavation depth of the foundation pit, which occurs at the intersection of the middle point of the oblique excavation line and the step distance section of the transverse excavation. Additionally, the lateral displacement increases closer to the excavation section. The lateral displacement of the envelope enclosure mainly depends on the relative constraint stiffness of the vertical and horizontal underground diaphragm wall of the foundation pit. The use of the ladder layered excavation method of slotting can effectively reduce the lateral displacement of the underground diaphragm wall. The simulated result and on-site monitoring result are nearly the same. These results can provide a corresponding theory and engineering basis for the selection of excavation methods for the same type of sand and pebble stratum foundation pit.

KEYWORDS

Sand and pebble geology, Deep foundation pit, Numerical simulation, Dynamic control, Lateral displacement

INTRODUCTION

With the rapid development of China's economy, the construction of urban rail transit has also achieved sustained and rapid development. During the construction of urban infrastructure such as the Chengdu Metro, unfavourable engineering geological conditions such as water-rich sand and pebble strata have brought greater difficulties to the construction of engineering foundation pits and have created technical problems that require solving. The geological conditions in Chengdu mostly consist of sand and pebble strata, and they are widely distributed. There are also large differences in the spatial distribution of the strata. Sand-pebble formations have a skeleton structure, a rich porosity, a large particle dispersion, almost zero cohesion, poor disturbance resistance, and easy water permeability. These strata are typical in mechanically unstable formations. During the excavation of foundation pits, due to insufficient research on this type of geological condition and unknown engineering characteristics, engineering accidents such as overall instability of the foundation pit and ground collapse are often caused. Therefore, it is of great theoretical and practical significance to study the dynamic construction control method of sandy pebble geological deep foundation pits.

Scholars have adopted different methods to study different approaches to engineering and technical problems in the excavation of deep foundation pits. Liao et al [1] used the field monitoring data of the shotcrete anchoring of a deep foundation pit in Chengdu to obtain the deformation law of deep foundation pits in Chengdu area and its influence range, and proposed a new type of supporting strength, stability calculation method and deformation control method for deep foundation pit. Yu et al [2] verified the necessity of 3D analysis for foundation pit engineering. Ou et al [3] gave the deformation characteristics of foundations pits for the Taipei soft soil area, while Wang et al [4] gave the deformation characteristics of foundation pits under soft soil conditions. Ou et al [5,6] explored the changes in the lateral movement of the wall and the settlement of the ground surface behind the wall in different regions and under different stratum conditions, as well as the characteristics of time and space. Tong et al [7] used the particle discrete element method to analyse the changes in the surrounding ground settlement during the excavation of the deep foundation pit. Finno et al [8] obtained the range of influence of the pit angle effect for the Chicago stratum. Feng et al [9] analysed the overall deformation of the subway station foundation pit in consideration of the spatial effects. Li et al [10] discussed the space-time laws of the ground subsidence, pile displacement, supporting axial force and pit bottom bulging of the foundation pit. Wang et al [11] established a numerical analysis model of the deep foundation pit supporting structure to analyse the settlement and deformation laws.

As can be seen above, there are few studies on the influence of the relative stiffness of the vertical and horizontal walls of the foundation pit on the lateral deformation of the retaining structure for the long-strip subway foundation pit in the water-rich area with sand and pebble geology. In addition, the general excavation of foundation pits usually only considers the impact of layered excavation on the lateral displacement of the underground diaphragm wall of the subway foundation pit, and there are few studies on the impact of soil excavation methods and support erection timing. At the same time, there is still a lack of systematic, comprehensive and detailed research on the dynamic construction control methods of deep foundation pits in sand and pebble geology. Therefore, using the FLAC 3D finite difference software, combined with the grooved stepped foundation pit excavation method, the deformation law of the underground continuous wall during the dynamic excavation of the foundation pit is analysed and studied; the relationship between the relative rigidity of the transverse wall and the longitudinal wall of the foundation pit is discussed; the influence of earth excavation method and support erection on lateral displacement of underground diaphragm wall of subway foundation pit is studied, which has important practical guiding significance for solving practical engineering problems.

Excavation method for the stepped sand-pebble layer of a deep foundation pit

This research relies on Jinfu Station of Chengdu Metro Line 6, the intermediate station of the first and second phases of the project. The foundation pit of the standard section of the station is 20 m wide, approximately 20.36-21.5 m deep and 311.3 m long. The half-cover digging construction method is adopted for construction, and the supporting system adopts a type of supporting pile + internal support. The support system for the excavation standard section of the foundation pit adopts a reinforced concrete support + three steel supports, and the diagonal wells are used at the end wells. The top of the pile is provided with a reinforced concrete crown beam, the first support is supported on the concrete crown beam, and the steel support is supported on the steel enclosure.

Vertical excavation method of the foundation pit sand-pebble layer

For the excavation of the vertical soil of the foundation pit, four layers of excavation were used. The first excavation reached the design elevation of the bottom of the first concrete support. The second excavation depth was 7.5 m, excavated for three times respectively, each excavation depth was 2.5 m; the third excavation depth was 6.0 m, excavated for three times respectively, each excavation depth was 2 m; the last excavation was excavated to the design base level. The specific excavation method of each layer is described as follows.

Excavation of the first layer of earthwork

The first layer of earthwork is excavated as a whole to form a plane at the bottom of the crown beam. After the template is installed, the first layer of the concrete support is poured. After the concrete support reaches the design strength, excavation from the north to the south is used to excavate the second layer of soil grooves. During the excavation, the support plane is reserved for the construction plane, ensuring the groove width in the middle of the foundation pit is 9 m. The soil on both sides of the steps is stable. A schematic diagram of the excavation section of the first layer of earthwork is shown in Figure 1.

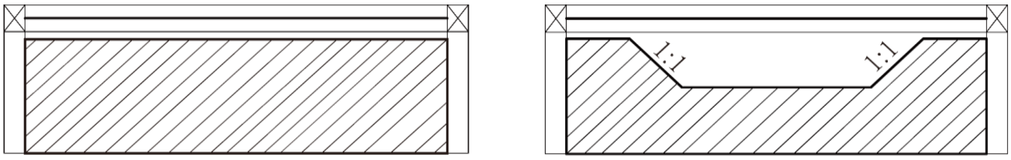

(a) Schematic diagram of horizontal section (b) Schematic diagram of vertical section

Fig. 1 – Schematic diagram of the excavation section of the first layer of earthwork

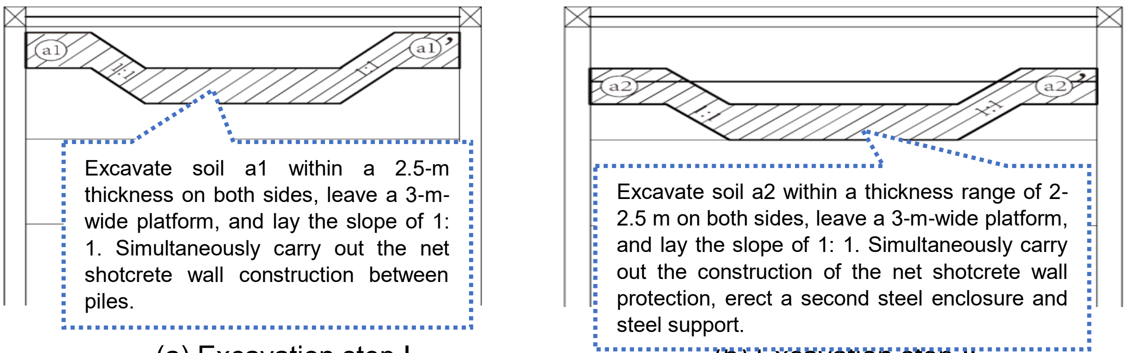

(a) Excavation step I (b) Excavation step II

Fig. 2 – Vertical concrete excavation diagram of the second layer of earthwork

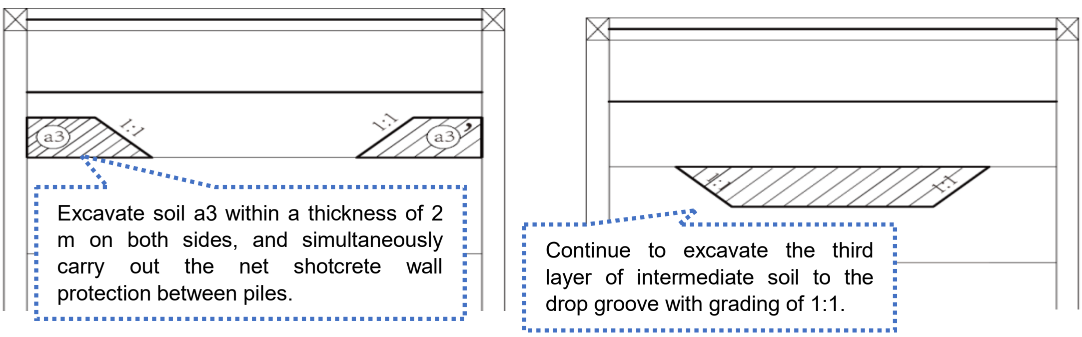

(c) Excavation step III (d) Excavation step IV

Fig. 2 – Vertical concrete excavation diagram of the second layer of earthwork

DOI 10.14311/CEJ.2020.03.0026

Excavation of the second layer of earthwork

The excavation depth of the second layer of earthwork is 7.5 m, which is excavated for three times, and each excavation depth does not exceed 2 ~ 2.5 m. The concrete vertical excavation of the second layer of earthwork is shown in Figure 2.

Excavation of the third layer of earthwork

The excavation depth of the third layer of earthwork is 6 m, which is excavated for three times, and each excavation depth does not exceed 2 m. The middle slot is excavated first in the horizontal direction, the sides of the slot are sloped at 1:1, and the soil in b1, b2, and b3 are excavated on both sides in sequence. Platforms with a width of 3 m are left on both sides of each excavation. Soil spraying is carried out on the soil platform. A third steel enclosure and steel support is erected after the b1 soil is excavated. A schematic diagram of the excavation section of the third layer of earthwork is shown in Figure 3.

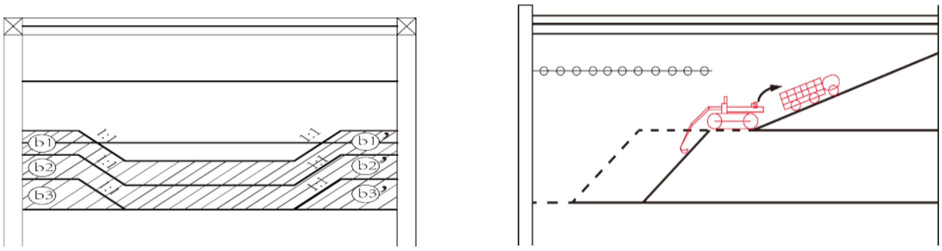

(a) Excavation step (b_1-b_1, b_2-b_2, b_3-b_3 part) (b) Mechanical operation diagram

Fig. 3 – Schematic diagram of the vertical excavation section of the third layer

Excavation of the fourth layer of earthwork

The excavation depth of the fourth layer of earthwork is 6.4 m, and it is excavated three times; each excavation depth does not exceed 2 ~ 2.4 m. The middle slot is excavated first in the horizontal direction, both sides of the slot are sloped at 1:1, and the soil in c1, c2, and c3 is excavated on both sides in sequence, leaving a 3 m wide platform on each side of the excavation. Soil spraying is carried out on the soil platform. Where the excavation reaches 300 mm above the ground of the foundation pit, manual excavation should be used to remove the remaining earthwork. Over-excavation is strictly prohibited to minimize disturbance to the foundation soil. A schematic diagram of the excavation section of the fourth layer of earthwork is shown in Figure 4.

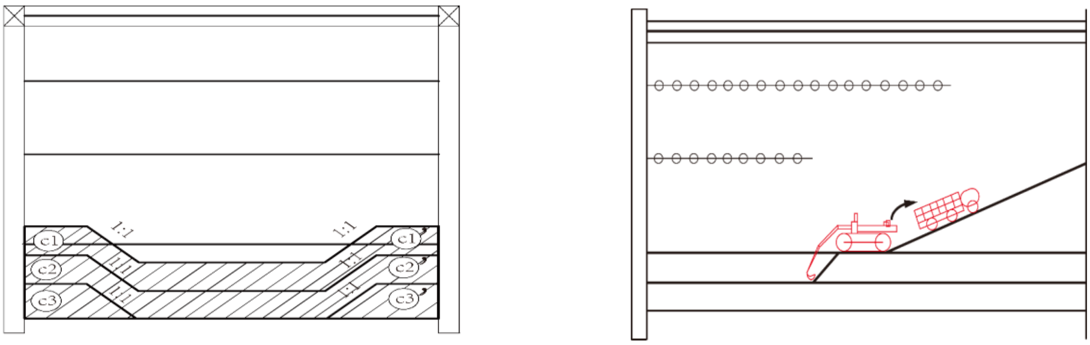

(a) Excavation step (c_1-c_1, c_2-c_2, c_3-c_3 part) (b) Mechanical operation diagram

Fig. 4 – Schematic diagram of the excavation section of the fourth layer of earthwork

MODELLING AND SIMULATION

Calculation parameters and models

The irregular and convex edge part of the foundation pit on the actual site is simplified to a regular rectangular end well. According to St. Venant's theorem, the model boundary is 5 times deeper than the excavation boundary of the foundation pit and 3 times deeper in the depth direction.

The parameters of Tables1~3 are derived from experience and engineering practice. The support is simulated using beam elements in Table 1, and the beam element parameters can be seen in Table 2; the plastic-hardening constitutive model, and the soil parameters of each layer can be seen in Table 3. During the excavation process, the precipitation process of the foundation pit is no longer considered. The final calculation model of the solid unit is 420 m × 140 m × 60 m.

Tab. 1 - Main parameters of the underground diaphragm wall

Diaphragm Wall	*E* /GPa	ν	Thickness *t* /m	ρ /(kg/m^3)	k_n /(N/m^3)
Inside	24.00	0.20	0.85	2500	1.8×10^{10}
Outside	24.00	0.20	0.85	2500	1.8×10^{10}
Diaphragm Wall	k_s/(N/m^3)	*c* /kPa	ψ /°	f_t /(N/m^2)	c_r /(N/m^2)
Inside	1.8×10^{10}	7.00	6.00	0.00	2500
Outside	1.8×10^{10}	14.00	12.50	0.00	2500

Tab. 2 - Support unit parameters

Support	Section size /mm	Density ρ /(kg/m^3)	*E* /GPa	Cross-sectional area *S*/m^2	I_y/m^4	I_z/m^4
RC Support	1200×1400	2500	25.0	1.68	0.2016	0.2744
Steel support	ϕ609 (t = 6)	7800	200	0.0298	1.32×10^{-3}	1.32×10^{-3}

Tab. 3 - Soil layer parameters of the plastic-hardening model

Model parameters	Miscellaneous fill [12]	Clay [12]	Sand [12]	Loose sand-pebble	Medium dense sand-pebble	Compact sand-pebble
p^{ref}/kPa	100.00	100.00	100.00	100.00	100.00	100.00
E_{50}^{ref}/MPa	6.00	8.00	30.00	27.27	20.07	14.86
E_{ur}^{ref}/MPa	18.00	24.00	90.00	109.07	80.29	59.44
E_{oed}^{ref}/MPa	6.00	4.00	30.00	8.19	11.12	10.10
υ_{ur}	0.20	0.20	0.20	0.20	0.20	0.20
c'/kPa	0.00	5.00	1.00	0.00	0.00	0.00
ϕ'/ °	15.00	25.00	32.00	26.05	34.65	42.05
ψ/ °	0.00	0.00	2.00	14.29	13.51	13.43
m	0.65	0.80	0.50	0.22	0.42	0.63
k_0^{nc}	0.44	0.50	0.47	0.56	0.43	0.33
R_f	0.90	0.90	0.90	0.34	0.79	0.90

Numerical simulation conditions

The site adopts the stepped excavation construction method of the slot, combined with the longitudinal excavation method, and according to the vertical excavation of the soil layer, the simulation conditions are set as shown in Figure 5. The first floor is excavated to the first concrete support design elevation position (R1), and the concrete support is applied. Then, after the groove excavation (R2) of the remaining soil layer is finished, the excavation of the remaining soil layer is performed from the lower left corner to the upper right corner according to the simulation condition setting table during the simulation. The excavation of each layer is divided into two steps. The first step is to excavate the slot (*Z) in the middle, and the second step is to clean up the steps (*B) on both sides. When excavating to the support design elevation, support erection is carried out in time. The excavation method of the entire foundation pit adopts a backward angled excavation method, and the foundation pit is excavated in turn.

CALCULATION RESULTS AND RESULTS ANALYSIS

To accurately obtain the lateral movement of the underground continuous wall during the stepped excavation of the slotted groove, when the fourth soil excavation in the first section reached the design elevation of the bottom of the foundation pit, data was recorded (the excavation simulation condition setting chart is the excavation condition of the top left corner without filling background). The data is recorded after each excavation (the excavation simulation condition setting chart shows the conditions of completing the same filling background colour). The names of the data are recorded as working conditions I ~ X, respectively.

Total excavation depth / m	Excavation number	Layer number	Layer depth / m	Excavation conditions									
21.3	First layer excavation	First floor	1.4	R1									
		Slot drawing		R2									
	Second layer excavation	a1	2.5	a11Z	a12Z	a13Z	a14Z	a15Z	a16Z	a17Z	a18Z	a19Z	a110Z
				a11B	a12B	a13B	a14B	a15B	a16B	a17B	a18B	a19B	a110B
		a2	2.5	a21Z	a22Z	a23Z	a24Z	a25Z	a26Z	a27Z	a28Z	a29Z	a210Z
				a21B	a22B	a23B	a24B	a25B	a26B	a27B	a28B	a29B	a210B
		a3	2.5	a31Z	a32Z	a33Z	a34Z	a35Z	a36Z	a37Z	a38Z	a39Z	a310Z
				a31B	a32B	a33B	a34B	a35B	a36B	a37B	a38B	a39B	a310B
	Third layer excavation	b1	2.0	b11Z	b12Z	b13Z	b14Z	b15Z	b16Z	b17Z	b18Z	b19Z	b110Z
				b11B	b12B	b13B	b14B	b15B	b16B	b17B	b18B	b19B	b110B
		b2	2.0	b21Z	b22Z	b23Z	b24Z	b25Z	b26Z	b27Z	b28Z	b29Z	b210Z
				b21B	b22B	b23B	b24B	b25B	b26B	b27B	b28B	b29B	b210B
		b3	2.0	b31Z	b32Z	b33Z	b34Z	b35Z	b36Z	b37Z	b38Z	b39Z	b310Z
				b31B	b32B	b33B	b34B	b35B	b36B	b37B	b38B	b39B	b310B
	Fourth layer excavation	c1	2.0	c11Z	c12Z	c13Z	c14Z	c15Z	c16Z	c17Z	c18Z	c19Z	c110Z
				c11B	c12B	c13B	c14B	c15B	c16B	c17B	c18B	c19B	c110B
		c2	2.0	c21Z	c22Z	c23Z	c24Z	c25Z	c26Z	c27Z	c28Z	c29Z	c210Z
				c21B	c22B	c23B	c24B	c25B	c26B	c27B	c28B	c29B	c210B
		c3	2.4	c31Z	c32Z	c33Z	c34Z	c35Z	c36Z	c37Z	c38Z	c39Z	c310Z
				c31B	c32B	c33B	c34B	c35B	c36B	c37B	c38B	c39B	c310B

Note: Z--Middle slotted soil; B--Step soil on both sides.

Fig. 5 – Setup diagram of the excavation simulation conditions

Horizontal displacement of the underground continuous wall in the x direction

The cross-sectional position diagram of the horizontal displacement data point in the X direction of the underground diaphragm wall is shown in the Figure 6.

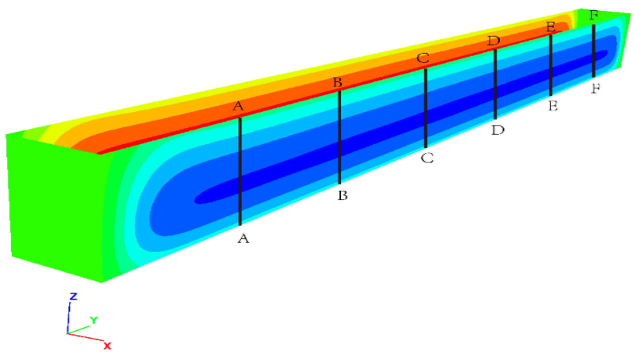

Fig.. 6 - Cross-section location of horizontal displacement data points in X direction of underground diaphragm wall

During the excavation of the foundation pit, to obtain the displacement change of the underground continuous wall in the x direction, six sections were taken as the data extraction surface, and the distance between adjacent sections was 50 m. The data obtained for each section is shown in Figure 7.

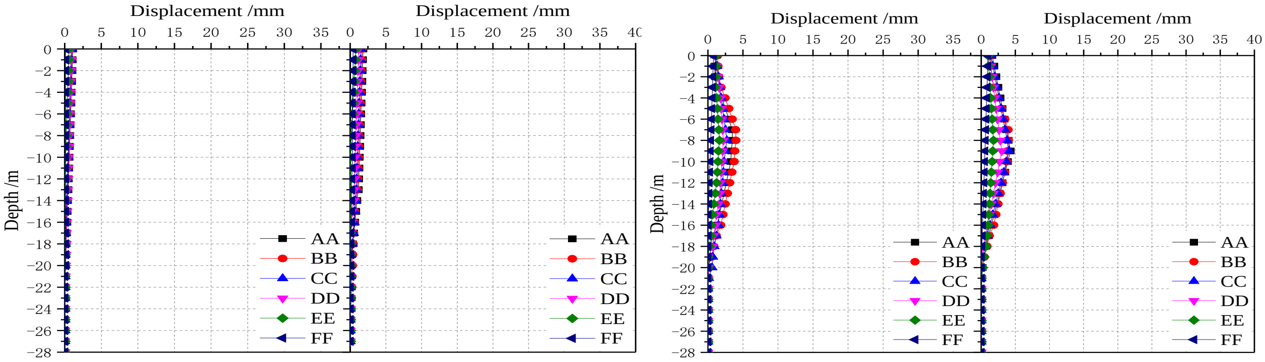

(a) Working condition I (b) Working condition II (c) Working condition III (d) Working condition IV

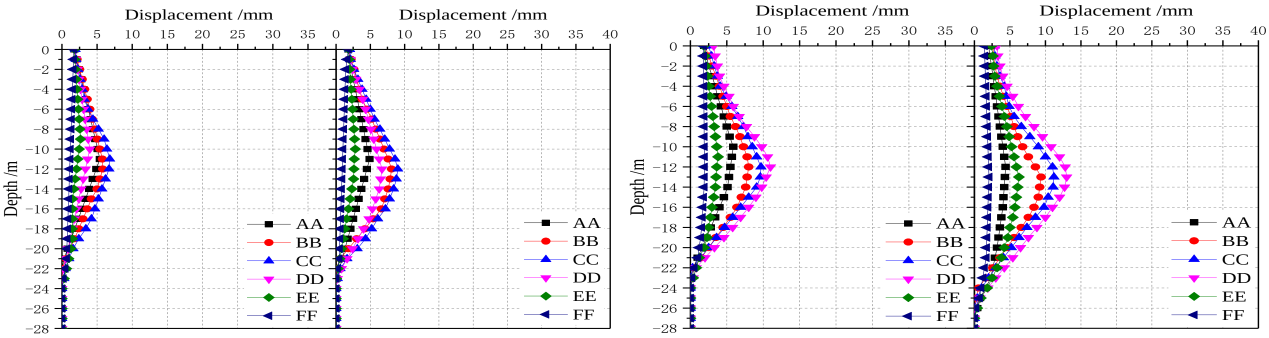

(e) Working condition V (f) Working condition VI (e) Working condition VII (f) Working condition VIII

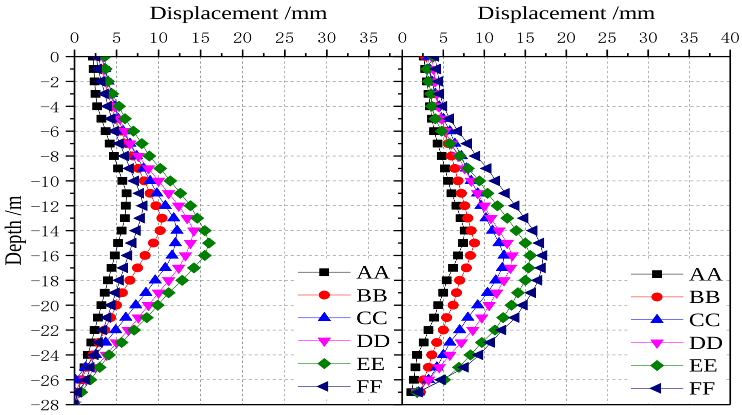

(e) Working condition IX (f) Working condition X

Fig. 7 – Horizontal displacement of the underground diaphragm wall in the x direction

It can be seen from Figure 7 that during the excavation of the foundation pit, the first and second working conditions were excavated to the design elevation of the foundation pit, and the entire foundation pit was excavated to a lesser extent. The difference in the earth pressure on both sides of the underground continuous wall was not sufficient to resist the embedded rigidity at the bottom of the underground continuous wall, and because of the stepped excavation of the slotted groove, the support was erected in time, and the maximum side shift was 2.2 mm. Later, inclined-angle retrogressive excavation was adopted, and the excavation construction step was 30 m. It can be seen from working conditions III and IV that as the excavation of the foundation pit gradually increased, the lateral movement of the underground continuous wall gradually increased, and the maximum moving section appeared at the intersection of the midpoint of the diagonal excavation line and the excavation section. Second, the maximum lateral displacement section was on the adjacent side of the maximum lateral displacement surface. The closer to the cross section of the lateral excavation construction step, the larger the lateral displacement was. The maximum lateral displacement was 4.8 mm. When the excavation reached working conditions V or VI, the excavation volume of the soil inside the foundation pit exceeded half of the total excavation volume of the soil. The difference in the earth pressure on both sides of the underground diaphragm wall gradually approached the bending resistance provided by the embedded end of the underground diaphragm wall, which caused the tendency of the underground diaphragm wall to rotate. The maximum excavation depth of the foundation pit was close to 16.9 m after the excavation to working conditions VII and VIII, and the supporting system was fully applied. The maximum lateral displacement of the underground continuous wall was 13.2 mm. When the excavation reached working conditions IX and X, the lateral movements of the underground continuous wall at section AA were almost equal, which indicates that the internal forces of the underground continuous wall were redistributed to reach a stable and relatively balanced state with each envelope system. The lateral movement of the underground continuous wall in the x direction was 17.6 mm.

Horizontal displacement of the underground continuous wall in the Y direction

The cross-sectional position diagram of the horizontal displacement data point in the Y direction of the underground diaphragm wall is shown in Figure 8.

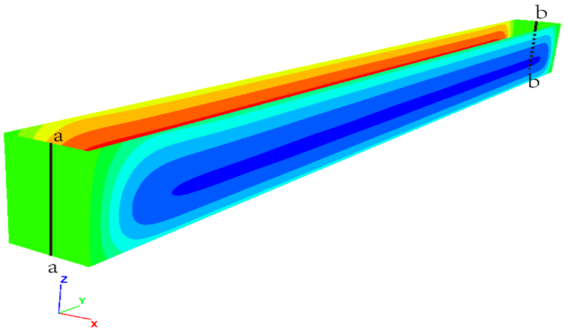

Fig. 8 - The position of the cross section of the horizontal displacement data point in the Y direction of the underground diaphragm wall

To obtain the deformation evolution mechanism of the horizontal underground diaphragm wall and to study the constraint of the horizontal wall of the end well of the foundation pit on the vertical underground diaphragm wall, the middle section is taken at the lateral wall on both sides, and the calculation results are shown in Figure 9.

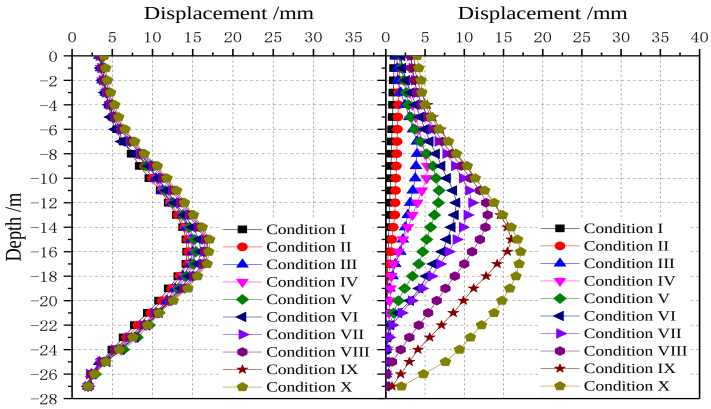

(a) Section a-a (b) Section b-b

Fig. 9 – Horizontal displacement of the underground diaphragm wall in the y direction

When extracting the result, the fourth condition soil in the first section has been excavated to the design elevation at the bottom of the foundation pit, and the lateral movement of its underground continuous wall has stabilized, as shown in Figure 9 (a). The minimum lateral displacement of the underground continuous wall in section a-a is 14.3 mm. During the gradual excavation of the foundation pit, the lateral displacement of the underground continuous wall gradually increases due to the redistribution of the internal forces of the underground continuous wall and its supporting system. The maximum lateral shift value is 17.1 mm. During the excavation process, the shape of the lateral shift curve of section a-a did not change. For section b-b, since the excavation of the soil is from the original unexcavated state until the excavation reaches the base design elevation, during the entire excavation process, when the excavation depth of the foundation pit is small, the bottom of the underground continuous wall has a larger embedded stiffness, the lateral deformation of the foundation pit retaining structure is similar to that of the "cantilever beam", and the maximum lateral displacement mainly occurs at the top of the wall, at approximately 1.1 mm. With the increase in the excavation depth, the position of the maximum displacement of the underground continuous wall gradually moves down. When the foundation pit is excavated to the first concrete design elevation, the first concrete support did not reach the design strength during construction. The overall rigidity of the foundation pit did not improve. Thus, the top lateral deformation of the retaining wall of the underground continuous wall of the foundation pit is completely determined by the longitudinal (horizontal) relative stiffness of the wall. With the increase in the excavation depth, it can be seen that the lateral stiffness of the retaining structure of the foundation pit is significantly stronger than that of the longitudinal side. The relative restraint effect along the wall is related to the excavation depth. The larger the longitudinal dimension of the foundation pit, the closer the plane deformation of the foundation pit to the plane strain state. During the subsequent excavation process, the height of the maximum lateral deformation of the underground continuous wall gradually develops from the top of the underground continuous wall to the deep soil. When excavated to the design elevation of the bottom of the foundation pit, the maximum lateral deformation in the y direction is 16.8 mm.

Analysis of on-site monitoring results of horizontal displacement of underground diaphragm wall

In order to verify the rationality of the numerical simulation result, the horizontal displacement of the underground diaphragm wall during the on-site excavation of the deep foundation pit was monitored and analysed. Therefore, the representative a-a section of the short side direction and b-b section of the long side direction of the deep foundation pit are selected to analyse the on-site monitoring data of underground diaphragm wall, and the change law curves are draw, as shown in Figure 10.

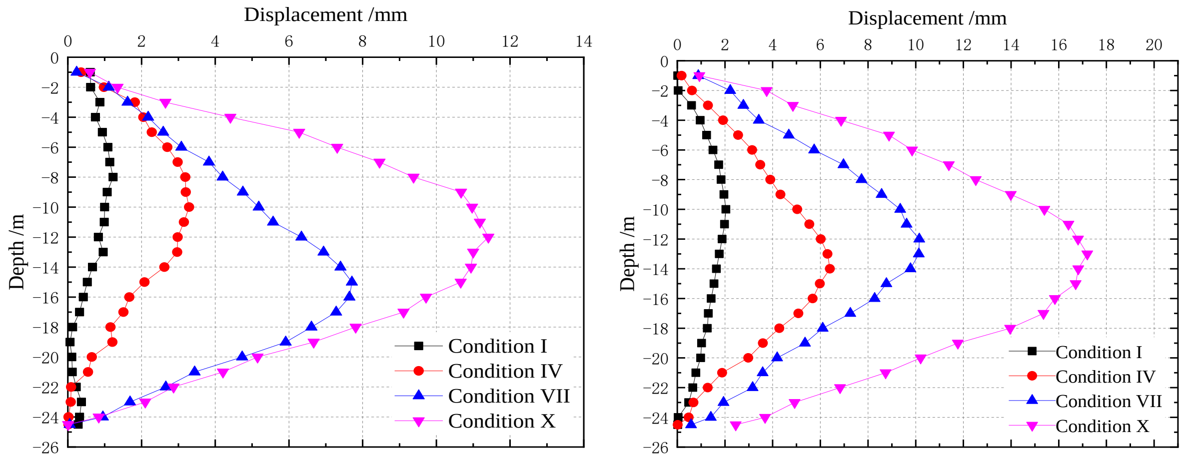

（a）Section a-a （b）Section b-b

Fig. 10 – On-site horizontal displacement of underground diaphragm wall

In Figure 10, it can be seen that when the excavation depth of the foundation pit is small, the lateral displacement value of the underground diaphragm is small. The maximum horizontal displacement of the diaphragm wall in the deep layer gradually decreases with the increase of the excavation depth of the foundation pit. The maximum value appears near the excavation surface. The deep horizontal displacement of the diaphragm wall shows a “big belly” shape. When the foundation pit is excavated to the designed bottom elevation, the maximum side displacement of a-a section of the short side about the foundation pit is 11.41 mm, the maximum side displacement of b-b section of the long side direction is 17.2 mm, and the side displacement of the long side of the foundation pit is much larger than that of the short side. It indirectly indicates that during the excavation of the foundation pit, the lateral displacement of the diaphragm wall mainly depends on the relative restraint stiffness of the diaphragm wall in the vertical and horizontal directions of the foundation pit.

Comparison and analysis of simulated result and on-site monitoring result

By analysing and comparing the numerical simulation value curves (Figure 7 and Figure 9) with the on-site monitoring value curve (Figure 10), it can be easily seen that during the construction process, the displacement of the underground diaphragm wall is small; and the change law of lateral displacement of the two changes consistently with the increasement of excavation depth, both appears as “big belly-shaped”; at the same depth, the displacement value error of the two is small, which verifies that the simulation calculation results are credible and proves the rationality of the numerical test method; meanwhile, it reveals that the stepped excavation construction method can effectively control the displacement of the underground continuous wall.

Grooved step construction control method

Combined with the previous studies of the research group, the overall layered foundation pit excavation method is adopted. When the foundation pit is excavated to the design elevation of the pit bottom, the maximum lateral displacement of the underground continuous wall is 28.5 mm, while the maximum lateral displacement of the underground continuous wall obtained by the stepped excavation construction method is 17.6 mm. Compared with the overall performance, the layered foundation pit excavation method reduces the maximum side shift by 38%. It can be concluded that during the excavation of the foundation pit, the stepped excavation of the groove is very effective in reducing the deformation of the foundation pit, and during the earthmoving process, the method of reserving steps on both sides of the foundation pit can be used for more than just subsequent erection. The support provides a good working surface and plays a beneficial role in controlling the lateral deformation of the foundation pit retaining structure. In the actual design of the foundation pit enclosure structure, the stiffness of the underground diaphragm wall can be appropriately reduced, and construction cost can be achieved through strict control of the construction technology.

CONCLUSIONS

For the simulation method during the excavation of the foundation pit, in order to reduce the calculation, cost in the simulation process, the overall layered excavation method is generally adopted. In this paper, we take the actual subway foundation pit Jinfu station as an example, combined with the actual construction conditions on site, adopting the grooved stepped excavation method, the finite difference software FLAC 3D is used to simulate the excavation process of the foundation pit. The simulated result and on-site monitoring result are nearly the same, which verifies the rationality of finite element method. The specific conclusions are drawn as follows:

1) During the excavation process, the larger the longitudinal dimension of the foundation pit, the closer the deformation evolution mechanism of the underground diaphragm wall to the plane strain problem. The grooved stepwise excavation method is adopted. As the excavation depth of the foundation pit gradually increases, the position of the maximum lateral displacement of the underground continuous wall gradually moves down and appears at the midpoint of the diagonal excavation line and the lateral excavation. As the cross position of the step section moves closer to the excavation section, the side shift becomes greater.

2) During the excavation of the foundation pit, the lateral constraint of the end well of the foundation pit is significantly greater than the longitudinal constraint. The lateral displacement of its retaining structure is mainly determined by the relative constraint stiffness ratio of the vertical and horizontal underground diaphragm wall of the foundation pit. In the past, the foundation pit has been simplified to consider the plane strain problem, which failed to correctly reflect the constraints provided by the end well on the vertical underground diaphragm wall, and the design was too conservative.

3) By comparing the simulated result and on-site monitoring result, it is found that the error between them is small, and their displacement changing trend law is very similar, verifying the reliability of simulation method.

4) The slotted stepwise layered excavation method can effectively reduce the lateral movement of the underground continuous wall by 38% compared with the overall excavation method. During the groove drawing process, the two side steps provide an effective working surface for the erection of the support.

ACKNOWLEDGMENTS

This research is supported in part by the Science and Technology Project in China Railway 21th Bureau Group Co. LTD. (Grant number: 17C-5).

REFERENCES

[1] Liao X.B., Chen Y., Zhu M., 1998. Design for anchor-shotcrete support structure and its application to protecting wall works of deep foundation pit in Chengdu area. The Chinese Journal of Geological Hazard and Control, Vol.9: 108-113. https://doi.org/10.16031/j.cnki.issn.1003-8035.1998.01.020

[2] Yu J. L., Gong X.N., 1999. Spatial behavior analysis of deep excavation. Chinese Journal of Geotechnical Engineering, Vol. 21: 21-25.

[3] Ou C., Hsieh P. G., Chou D. C., 1993. Characteristics of ground surface settlement during excavation. Canadian Geotechnical Journal, Vol.30, 758-767. https://doi.org/10.1139/t93-068

[4] Wang J.H., Xu Z.H., Wang W.D., 2007. Analysis of deformation behavior of deep excavations supported by permanent structure. Chinese Journal of Geotechnical Engineering, Vol. 29: 1899-1903.

[5] Ou C.Y., Chiou D.C., Wu T.S.,1996. Three-dimensional finite element analysis of deep excavations. Journal of Geotechnical Engineering, Vol. 122: 337-345. https://doi.org/10.1061/(ASCE)0733-9410(1996)122:5(337)

[6] Wang J. H., Xu Z. H., Wang W. D., 2010. Wall and ground movements due to deep excavations in shanghai soft soils. Journal of Geotechnical and Geoenvironmental Engineering, Vol.136: 985-994. https://doi.org/10.1061/(ASCE)GT.1943-5606.0000299

[7] Tong J.J., Wang M.N., Yu L., et al., 2014. A study of the land subsidence around the deep foundation pit of the Chengdu subway station. Hydrogeology & Engineering Geology, Vol. 42:97-101. https://doi.org/10.16030/j.cnki.issn.1000-3665.2015.03.16

[8] Finno R.J., Blackburn J. T., Roboski J. F., 2007. Three-dimensional effects for supported excavations in clay. Journal of Geotechnical and Geoenvironmental Engineering, Vol.133: 30-36. https://doi.org/10.1061/(ASCE)1090-0241(2007)133:1(30)

[9] Feng C. L., Zhang D.L., 2018. The general deformation mode and its application of subway station foundation pit in sandy cobble stratum. Chinese Journal of Rock Mechanics and Engineering, 37:4395-4405. https://doi.org/10.13722/j.cnki.jrme.2018.0722

[10] Li S., Zhang D.L., Shao Y.D., 2019. Research on spatio-temporal law of deep excavation deformation under complicated environment in Beijing Subway Station. Journal of Beijing Jiaotong University, Vol. 43: 29-36. https://doi.org/10.11860/j.issn.1673-0291.20190040

[11] Wang M.N., Zeng Z.Q., Zhao Y.T., et al., 2019. Study on deformation rules of earth's surface and support structure for deep foundation pit in bad gradation pebble stratum. Journal of Railway Science and Engineering, Vol.16: 646-653. https://doi.org/10.19713/j.cnki.43-1423/u.2019.03.012

[12] Brinkgreve R.B.J., Engin E., Swolfs W.M., et al., 2013. PLAXIS 3D 2013 User's Manuals, The Netherlands: Plaxis BV, Delft.